Journal of Applied Polymer Science

Design of Cyanate Ester/Azomethine/ZrO_2 Nanocomposites High-k Dielectric Materials by Single Step Sol-Gel Approach

Mathivathanan Ariraman, Ramachandran Sasi kumar, Muthukaruppan Alagar
Polymer Composites Lab, Department of Chemical Engineering, A.C. Tech, Anna University, Chennai-600 025, Tamil Nadu, India
Correspondence to: M. Alagar (E-mail: mkalagar@yahoo.com)

ABSTRACT: In this article we designed a cyanate ester based novel hybrid nanocomposites by sol–gel approach with different weight percentages of Zirconium dioxide (ZrO_2). The synthesized monomer and polymer nanocomposites were characterized by Fourier-transform infrared, ^1H, and ^{13}C nuclear magnetic resonance (NMR) spectra. Optical and thermal properties reveals the excellent optical transparency and good thermal stability of hybrid nanocomposites. Scanning electron microscope and high resolution transmission electron microscope analysis confirm the homogeneous dispersion of ZrO_2 in the nanocomposites. Interestingly 7% ZrO_2 nanocomposite exhibit highest k value of 9.21 which may be due to the well dispersion of ZrO_2 and their strong interfacial polarization in the organic–inorganic hybrid nanocomposites. © 2014 Wiley Periodicals, Inc. J. Appl. Polym. Sci. **2014**, *131*, 41097.

KEYWORDS: composites; copolymers; dielectric properties; differential scanning calorimetry (DSC)

Received 26 March 2014; accepted 7 June 2014
DOI: 10.1002/app.41097

INTRODUCTION

The continued miniaturization and ultra fast performance of the electronic devices requires advanced integrated circuits (IC).[1] It is well known that the high dielectric constant materials are essential to fabricate efficient products for consumer electronic devices. For nanoscale device fabrication, it is important to develop novel functional high k materials with excellent processing characteristics.[2] In this view, significant efforts have been focused on various polymeric matrices through epoxy,[3] polybenzoxazine,[4] cyanate ester,[5] and their composites as well. Among various polymer matrices, cyanate ester has been demonstrated and used for multifunctional applications.[6] Unique features of cyanate ester such as good thermo-mechanical and excellent dielectric properties greatly enhance their application to many commercial appliances. An exclusive of the above, is that it has low dielectric constant and loss, low moisture uptake, excellent flame retardant, and environmental compatibility.[7] In advantages of this, it could be expected that the cyanate ester and composites are to be the desirable low cost material for high dielectric applications. Thus, cyanate ester based material offers a wide platform to fabricate the printed-wiring circuit boards, thin cards, multichip module laminates, and sheet-molding compounds.

Recently, the cyanate ester-ceramic composites have been investigated for low k as well as high k dielectrics. It was observed that the hybridization of inorganic components with organic matrix significantly influences in dielectric nature due to their intrinsic behaviors. Many investigations in cyanate ester demonstrate that the addition of carbonaceous materials tunes the dielectric constant of the composites significantly.[8] Widely, the composites of cyanate ester with carbon nanotubes,[9] expanded graphite/CNT,[2,8] AlN/MCNT/cyanate ester have been investigated for high performance dielectric applications.[10] The major drawback in CNT/polymer composite materials are their aggregation even at lower concentration due to the strong inter-tubular Van der Waal's forces of attraction and that directly influences on the dielectric features.[8] However, the values of dielectric constants are still needed to be improved. In this context, an incorporation of nanosized ceramic components like SiO_2,[11] Zirconium dioxide (ZrO_2),[12] POSS,[13] SBA-15,[14] and $BaTiO_3$[15] are used instead of carbonaceous materials to stabilize the dielectric values by forming homogenous network without altering their physical nature of the host. Nanoceramic components with high dielectric constant and thermal stability are desirable for high k dielectric composites. In this view, ZrO_2 has excellent thermal and interfacial properties with very high dielectric constant (~25).[12] Hence, it is expected that the addition of ZrO_2 to cyanate ester could enhance the dielectric constant and thermal stability for on-board circuit applications.

In the present study an attempt has been made to develop hybrid composites based on ZrO_2 reinforced cyanate ester-azomethine to enhance the dielectric constant with high thermal stability, which is required for high performance applications.

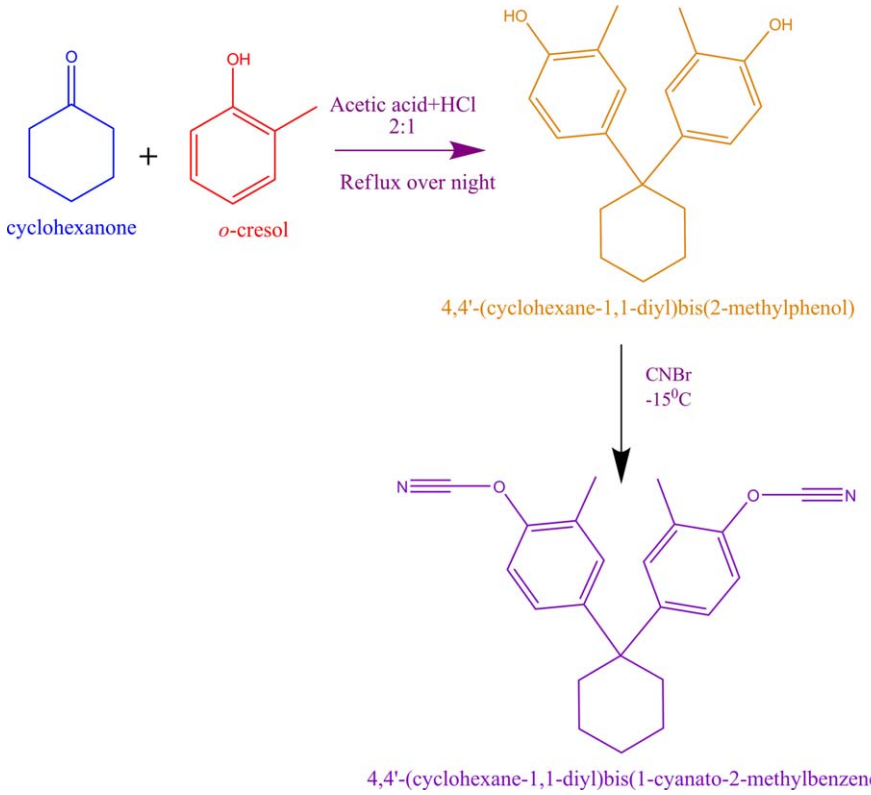

Scheme 1. Preparation of Cy-OCN monomer. [Color figure can be viewed in the online issue, which is available at wileyonlinelibrary.com.]

With this view, modified cyanate ester/azomethine diol/ZrO_2 nanocomposites have been prepared through sol–gel method. Typical polarization mechanism of triazine and azomethine with zirconia were investigated in relevant to the dielectric constant and thermal stability.

EXPERIMENTAL

Materials

Analytical grades of cyanogen bromide, 4-hydroxybenzaldehyde, zirconium isopropoxide, and 3-(glycidyloxypropyl)trimethoxysilane (GPTMS) were purchased from Spectrochem, India and

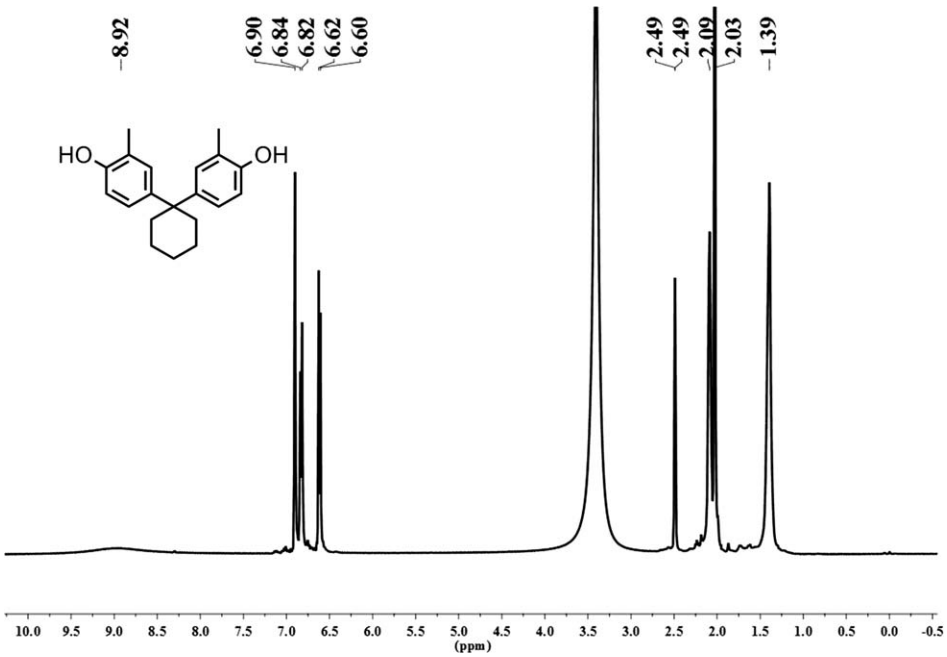

Figure 1. ^{1}H NMR spectra of Cy-OH.

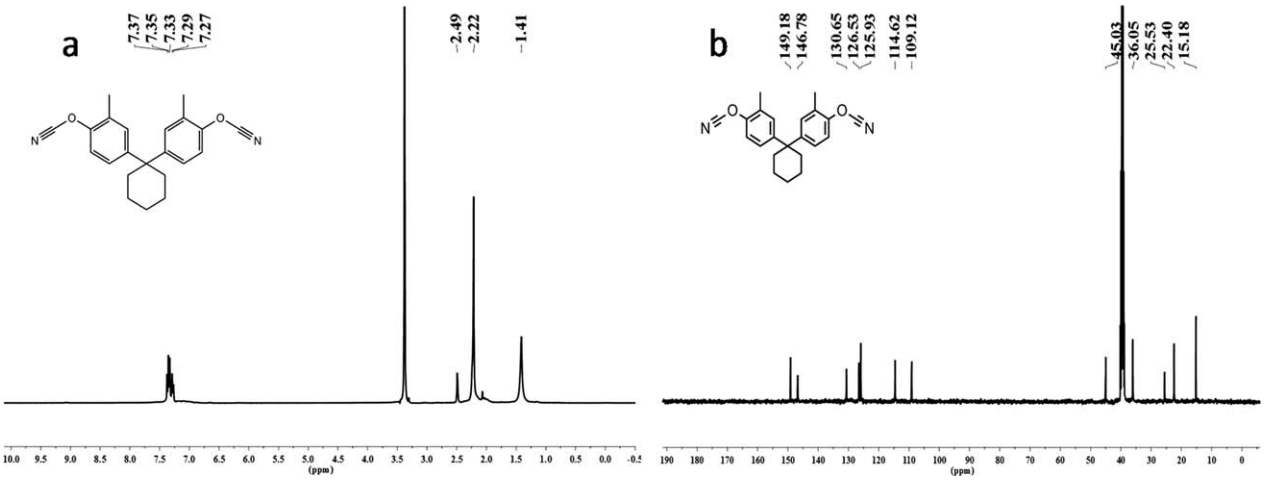

Figure 2. (**a**) ^{1}H NMR spectra of Cy-OCN, (**b**) ^{13}C NMR spectra of Cy-OCN.

Sigma Aldrich, respectively. Triethylamine, cyclohexanone, O-cresol, sodium hydroxide, acetic acid, *p*-Toluenesulfonic acid, and other solvents were purchased from SRL, India and were used as received without further purification.

Synthesis of 4,4′-Cyclohexane-1,1-diylbis (2-methylphenol) (Cy-OH)

Cy-OH was synthesized by the procedure as reported.[16] Cyclohexanone was added to a solution of O-cresol in the mixture of acetic acid and hydrochloric acid (2 : 1), and stirred for 5 h at 50°C. After the completion of reaction [monitored by thin layer chromatography (TLC)], cold water was added to the reaction mixture. The precipitate was washed several times with water and purified by acid–base treatment to yield 81% off white solid.

^{1}H nuclear magnetic resonance (NMR) ($CDCl_3$, δ, ppm): 8.92 (—OH), 6.90–6.60 (aromatic protons) 2.49–2.03 (cycloaliphatic protons), 1.39 (methyl proton).

Synthesis of Cyclohexane-1,1-diylbis-2-methylbenzene-4,1-diyl dicyanate (Cy-OCN)

The synthesis of Cy-OCN is as follows; Cy-OH was dissolved in dry acetone under nitrogen atmosphere and then the solution of cyanogen bromide in acetone was added, followed by the slow addition of triethyl amine at −15°C. After that the temperature was slowly raised to room temperature and stirred for 1 h. Subsequently, the reaction mixture was filtered and it was added to cold water, forming the precipitate immediately. The precipitate was washed several times with water and dried for 12 h at 70°C to yield 88% pale yellow solid.

Fourier-transform infrared (FTIR) (KBr cm^{-1}): 2923 (symmetric stretching), 2854 (cyclohexyl CH_2 asymmetric stretching), 2238 (CN vibration stretching).

^{1}H NMR ($CDCl_3$, δ, ppm): 7.37–7.27 (aromatic protons), 2.49–2.22 (cycloaliphatic protons), 1.41 (methyl protons).

^{13}C NMR ($CDCl_3$, δ, ppm): 149.18 (OCN), 146.78, 130.65, 126.53, 125.93, 114.62, 109.2 (aromatic carbon), 45.03, 36.05, 22.53, 22.40, 15.18 (aliphatic carbon).

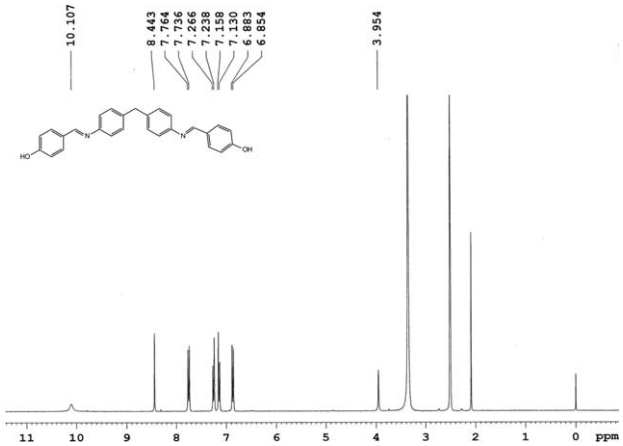

Figure 3. ^{1}H NMR spectra of AM-OH.

Synthesis of Azomethine Based diol (AM-OH)

4,4′-Diaminodiphenylmethane (1 mol) and 4-hydroxybenzaldehyde (2.2 mol) were dissolved in methanol, followed by addition of catalytic amount of PTSA to the reaction mixture and refluxed for 3 h. The formation of precipitate infers the product formation and also was monitored by TLC. After the completion of reaction the precipitate was filtered and the solid product was recrystallized with methanol to yield 83% pale yellow solid product.

FTIR (KBr cm^{-1}): 1600 (C═N stretching), 3200 (strong broad peak for phenolic "OH").

^{1}H NMR (DMSO, δ, ppm): 10.10 (OH), 8.44 (CH═N—), 7.75–6.85 (aromatic), 3.95 (—CH_2—).

Preparation of Cy-OCN/AM-OH/ZrO_2 Nanocomposites

The Cy-OCN/AM-OH/ZrO_2 nanocomposites with different concentration of ZrO_2 were prepared through sol–gel method. To a clear solution of Cy-OCN and AM-OH in THF, GPTMS was added and stirred for 15 minutes at 30°C. Subsequently, 0.1*N* HCl was added to the reaction mixture followed by the addition of various weight percentages (1%, 3%, 5%, 7%, and 10%) of zirconium isopropoxide. The resulting viscous solution was poured into the respective glass mould and the solvent was evaporated at 50°C for 3 h; and the temperature was raised slowly to 210°C at a

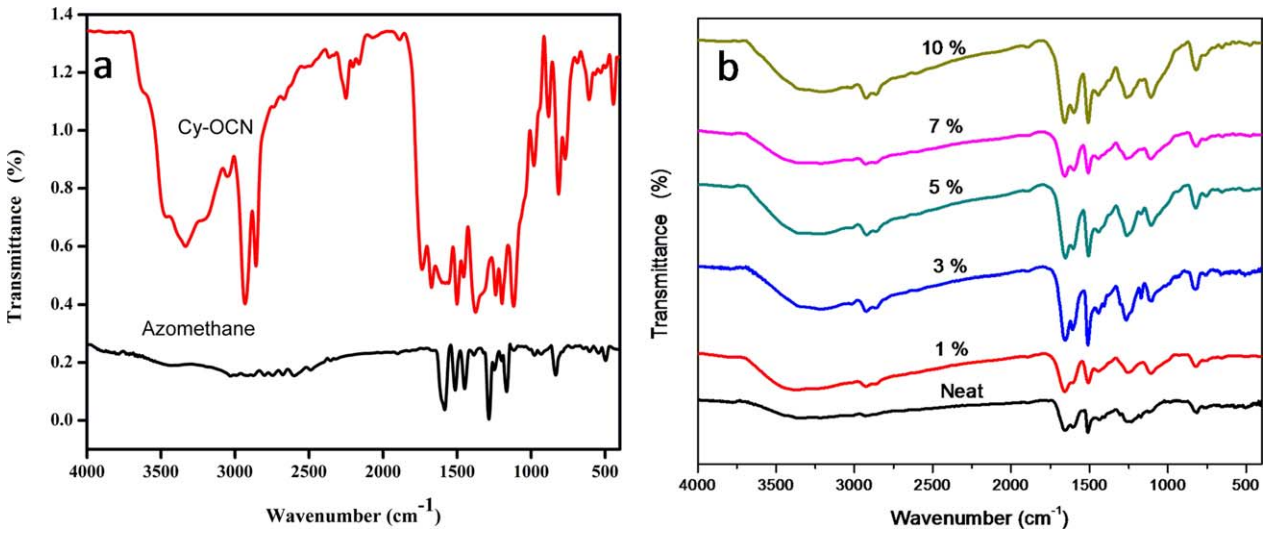

Figure 4. (**a**) FT-IR spectra of Cy-OCN and AM-OH. (**b**) FT-IR spectra of polymeric composites. [Color figure can be viewed in the online issue, which is available at wileyonlinelibrary.com.]

heating rate of 20°C/h. Further the cured films were peeled off and directly were used for characterization.

Characterization

FTIR spectroscopic measurements were conducted on a Bruker (TENSOR 27) using KBr pellet method. ^{1}H and ^{13}C NMR spectra were recorded on a Bruker 500 NMR spectrometer. The calorimetric analysis of the nanocomposites were performed on a Netzsch DSC-200 differential scanning calorimetry (DSC) at a heating rate of 10°C min^{-1} under nitrogen atmosphere. Thermogravimetric measurements were carried out on a Netzsch STA 409 thermogravimetric analyzer. The samples (about 10 mg) were heated from an ambient temperature to 750°C under a continuous flow of nitrogen (20 mL/min), at a heating rate of 10°C/min.

High resolution transmission electron microscope (HRTEM) analysis was carried out on TECNAI-G^2 (model T-30) at an accelerating voltage of 300 kV. Scanning electron microscope (SEM) measurements were performed on HITACHI S-3000H scanning electron microscope. A piece of film was fixed in the surface of the double-sided adhesive tape, and the film was sputtered with gold prior to SEM observation. Energy-dispersive spectroscopy (EDS) was performed on EDS DX-4 energy diffraction spectrometer and percentages of elements were observed. Dielectric constant was determined by Broad band Dielectric Spectrometer (BDS), NOVOCONTROL Technologies GmbH & Co. (model Concept 80) at 30°C in the range of 1 Hz–1 MHz. Optical transparencies of the polymeric nanocomposite film were characterized by shimadzu UV-2450 UV−visible spectrometer.

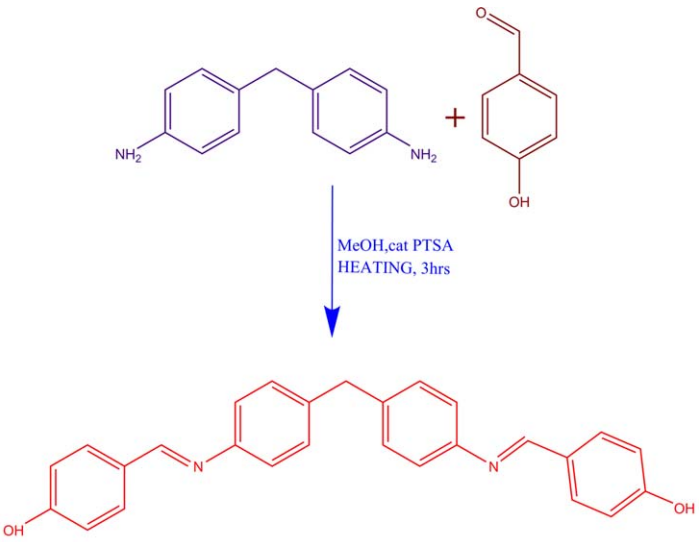

4,4'-(1*E*,1'*E*)-(4,4'-methylenebis(4,1-phenylene)bis(azan-1-yl-1-ylidene))bis(methan-1-yl-1-ylidene)diphenol

Scheme 2. Preparation of AM-OH monomer. [Color figure can be viewed in the online issue, which is available at wileyonlinelibrary.com.]

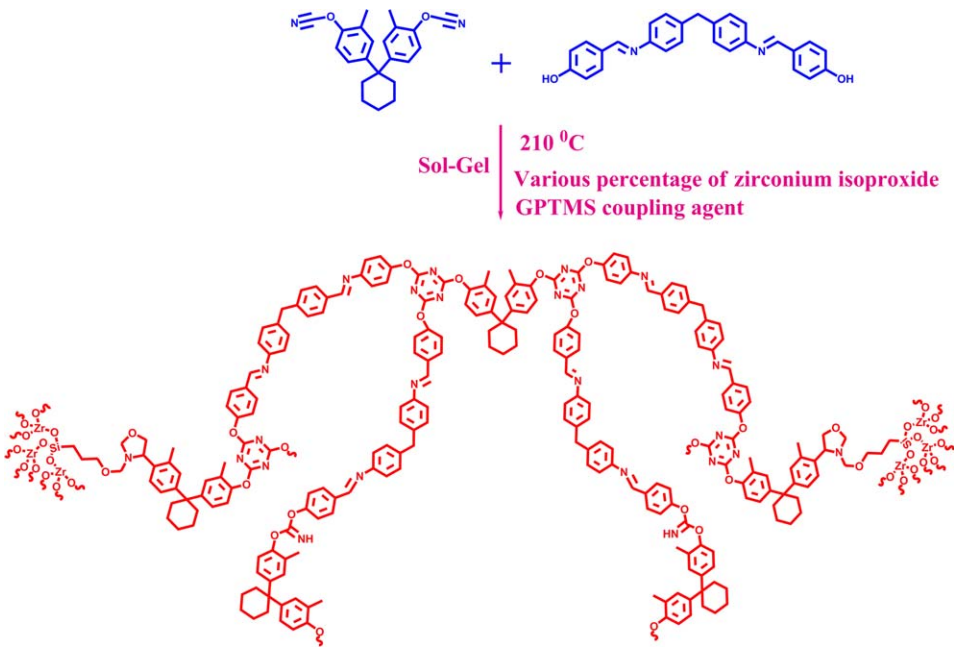

Scheme 3. Schematic representation of cyanate ester-azomethine nanocomposites formation. [Color figure can be viewed in the online issue, which is available at wileyonlinelibrary.com.]

RESULT AND DISCUSSION

Characterization of Cy-OH and Cy-OCN

The formation of 4,4′-cyclohexane-1,1-diylbis(2-methylphenol) (Scheme 1) was confirmed by ^{1}H NMR as shown in Figure 1. The appearance of peaks at 8.92 ppm and 2.49–2.03 ppm represents the hydroxyl and aliphatic cyclohexyl protons, respectively. The ^{1}H, ^{13}C NMR, and FTIR spectra further support the successful formation of cyanate ester. The disappearance of peak at 8.92 ppm in ^{1}H NMR and the presence of peak at 149.18 ppm related to OCN in ^{13}C NMR demonstrate the formation of Cy-OCN. In addition, the presence of vibrational band at 2238 cm^{-1} in FTIR spectra indicates the formation of cyanate ester (Figure 2).

Characterization of AM-OH

The synthesized Schiff base diol was confirmed by ^{1}H NMR and FTIR spectra. The ^{1}H NMR shows peaks (Figure 3) at 10.10 and 8.44 ppm corresponding to the hydroxyl and azomethine groups, respectively. FTIR spectrum shows [Figure 4(a)] the bands due to OH and C═N at 3200 and 1600 cm^{-1}, respectively, which confirms the formation of azomethine diol (Scheme 2).

Characterization of Cy-OCN/AM-OH/ZrO_2 Polymer Nanocomposites

The sol–gel synthesis of Cy-OCN/AM-OH/ZrO_2 nanocomposites is shown in Scheme 3 and the formation of nanocomposites was further confirmed by FTIR [Figure 4(b)] spectra. The appearance of bands at 1350, 1604 cm^{-1} and the broad band at 3400 cm^{-1} corresponding to triazine ring[11] and imidocarbonate, respectively, and also the disappearance of bands at 2238 cm^{-1} indicates the polymerization between respective OCN in cyanate ester and OH of azomethine monomer. The GPTMS is used as coupling agent, which forms Oxazoline between the monomers, which is

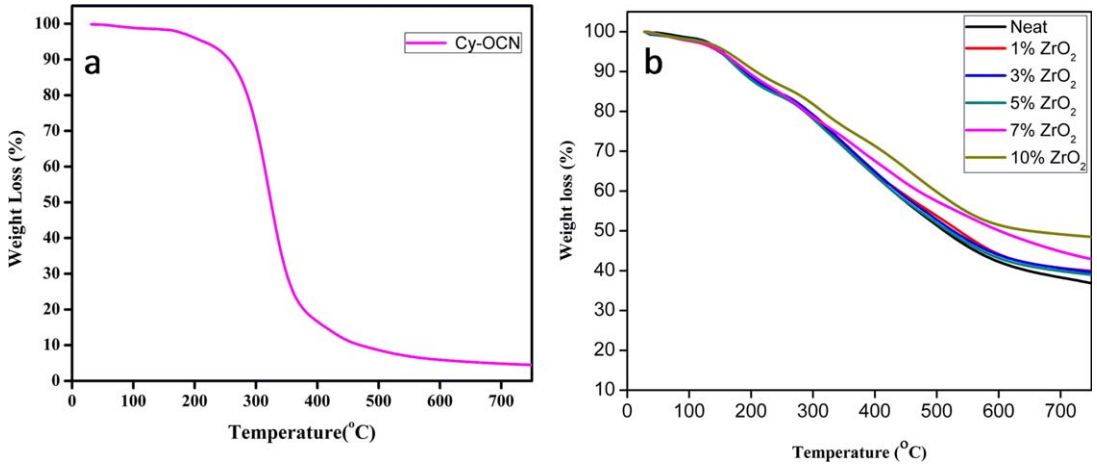

Figure 5. (**a**) TGA thermogram of Cy-OCN. (**b**) TGA thermogram of polymeric nanocomposites. [Color figure can be viewed in the online issue, which is available at wileyonlinelibrary.com.]

Table I. Thermal and Dielectric Properties of Polymeric Nanocomposites

Experiment	Char yield (@ 750°C) %	Dielectric constant (ε')	Dielectric loss Tan delta
Cy-OCN	4.22	3.22	0.0034
Cy-OCN/AM-OH	36.5	4.09	0.0075
Cy-OCN/AM-OH/ZrO_2 1%	38.9	5.92	0.0068
Cy-OCN/AM-OH/ZrO_2 3%	39.1	6.93	0.0080
Cy-OCN/AM-OH/ZrO_2 5%	39.6	7.36	0.0075
Cy-OCN/AM-OH/ZrO_2 7%	42.9	9.21	0.0088
Cy-OCN/AM-OH/ZrO_2 10%	48.4	7.50	0.0113

confirmed from the appearance of band at 1661 cm^{-1} in the FTIR spectra. Further additional band at 985 cm^{-1} indicates the successful incorporation of zirconia through covalent (Zr—O—Si) bond into the polymer composites.[17]

Thermal Properties

The thermal stability of Cy-OCN/AM-OH/ZrO_2 nanocomposites was investigated using thermogravimetric analysis (Figure 5). Figure 5(a) shows thermal stability of Cy-OCN polymer. The weight loss occurrence below 200°C represents the removal of adsorbed moisture and trace amount of solvents. Above 300°C the major weight loss associates to the destruction of triazine ring network and the formation of low molecular weight volatile organic components. In Figure 5(b), it explains the thermal stability of cyanate ester copolymer and the effect of ZrO_2 nanoparticles incorporation. It was observed that the copolymerized Cy-OCN/AM-OH is thermally more stable when compared with Cy-OCN polymer. Typical char yield percentage is given in Table I and it ascertains the improved thermal stability. Mostly, azomethine compounds are thermally more stable[18] and has been copolymerized with cyanate ester which increases the thermal stability. The thermal stability of polymer nanocomposites gradually increases, with increasing the weight percentages of ZrO_2 from 1% to 10% as shown in Figure 5(b). Figure 6 shows the DSC spectra of neat cyanate ester matrix, azomethine co-polymerized cyanate ester, and different weight percentages of ZrO_2 reinforced cyanate ester composites. From DSC profile it can be observed that all the nanocomposites exhibit the absence of exothermic peak associated to the curing, which describes the complete polymerization of nanocomposites as that of neat matrix.

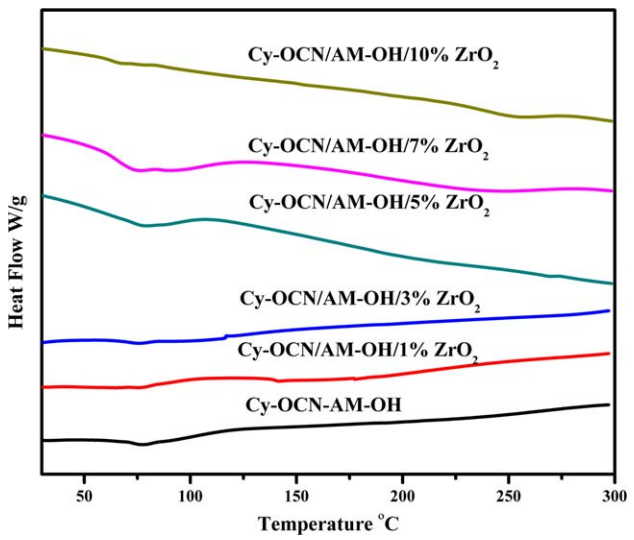

Figure 6. DSC curve of neat Cy-OCN/AM-OH and Cy-OCN/AM-OH/ZrO_2 nanocomposites. [Color figure can be viewed in the online issue, which is available at wileyonlinelibrary.com.]

Morphology

The surface morphology of Cy-OCN/AM-OH/ZrO_2 (7%) nanocomposites was characterized by HRTEM. Figure 7(a) shows the presence of ZrO_2 within the polymer matrix. It is found that the average size of the particles were approximately 30 nm. The occurrence of interfacial interaction between ZrO_2 and polymer matrix was well demonstrated from the TEM images represented in Figure 7(c). The dark spot represents the Zirconium oxide nanoparticles with polymer background. The corresponding SAED pattern describes the dispersion of polycrystalline ZrO_2 over the polymer matrix [Figure 7(d)]. The surface observation for neat Cy-OCN/AM-OH and Cy-OCN/AM-OH/ZrO_2 (7%) are shown in Figure 8(a,b) that indicates the well dispersion of ZrO_2 over the surface which is not visible in the neat polymer. The surface cavities can be seen which may be arised during the curing process and mainly associated to the evaporation of unreacted precursor and solvents. The elemental composition of ZrO_2 was confirmed for 7% Cy-OCN/AM-OH/ZrO_2 by EDS analysis and is shown in Figure 8(c,d). From the spectral data it was found that the appropriate concentration of Zr, O, and other polymer back bones are presented in the composites.

Optical Transparences of Polymer Nanocomposites

UV–visible spectra of Cy-OCN/AM-OH/ZrO_2 polymeric nanocomposites are shown in Figure 9. Optical transmission of composites depends on several parameters, namely the size of the inorganic domains, concentration of particles, refractive index difference between the particles and polymer matrix, and thickness of the films studied.[19] The cyanate ester compound optical transparency is very low (~62%) in the visible region. Interestingly, the addition of ZrO_2 enhances the optical transparency of the composites. The neat polymer shows the minimum transparency of 32% at 400 nm, and further increases to 71% at 800 nm. By adding the ZrO_2, the optical transparency increases to 40%–81% for 1% and 10% ZrO_2, respectively. This optical transparency resulted from the reflection losses of air gap in the film, and polymer/filler interfaces. Therefore the optical scattering in the composites are mainly due to the surface roughness and grain boundaries of the composites.[20]

Dielectric Properties

The dielectric behavior of the composite materials with respect to the frequency dependent was carried out. The dielectric constant of neat cyanate ester matrix was found to be 3.2 and the corresponding dielectric loss is approximately 0.003 at 1 MHz (Figure 10). As predicted, the neat cyanate ester matrix exhibits low dielectric constant and dielectric loss. It is known that the dielectric materials with high-k as close to the semiconductor

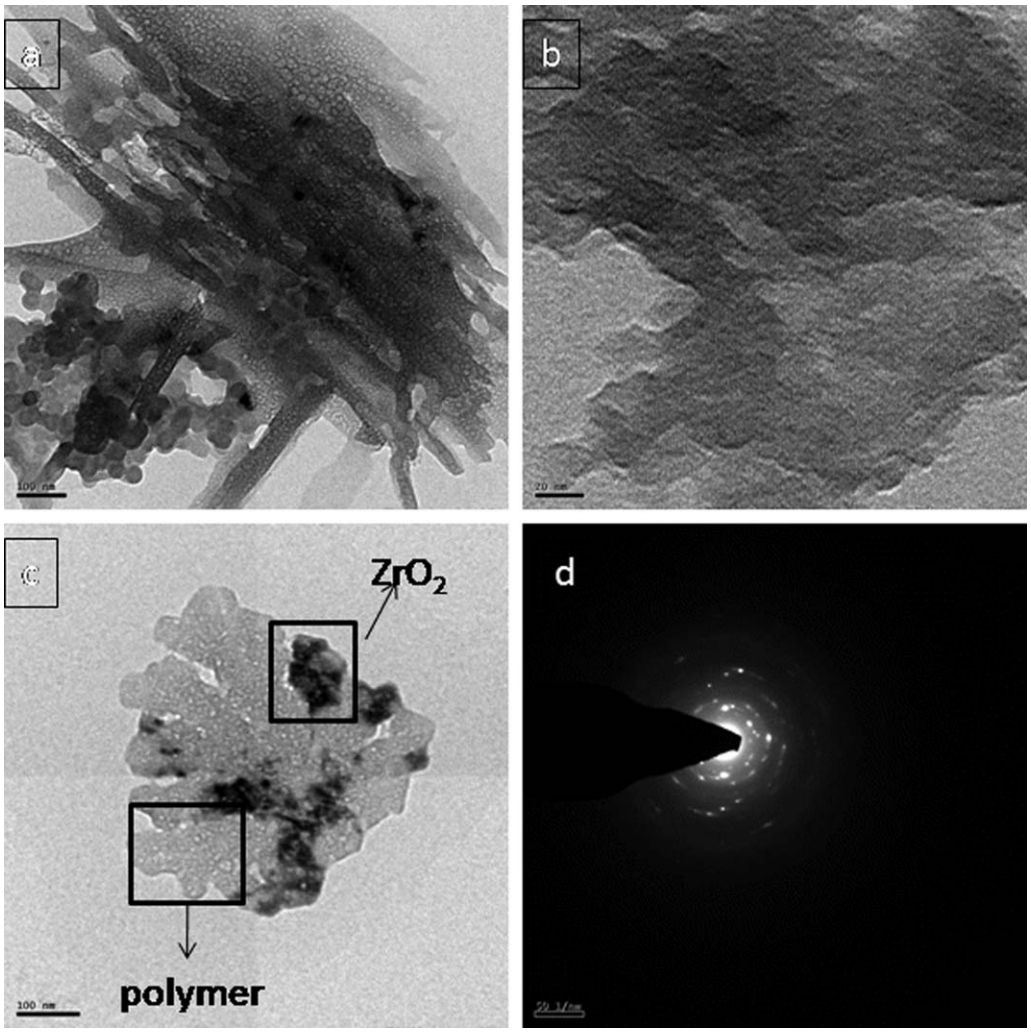

Figure 7. HRTEM images of 7% Cy-OCN/AM-OH/ZrO_2 nanocomposites.

will acts as a good conductor. The electron hopping within the dielectric material facilitates for charge dipole formation thereby conducting the electricity.[21] In particular the dielectric property of polymeric composites mainly depends on two factors such as distribution of electrical conductor and their interfacial polarity.[10]

Dielectric behaviors of Cy-OCN/AM-OH/ZrO_2 composites are represented in Figure 11(a). The values of dielectric constant and dielectric loss are represented in Table I. The value of dielectric constant was gradually increased with the increasing concentration of ZrO_2 when compared with that of neat polymer matrix. The observed dielectric constant values are in the range of 5.92–9.21 for loading of ZrO_2 concentration between 1% and 7%. Further increasing the ZrO_2 concentration to 10% the corresponding dielectric constant slipped to 7, owing to agglomeration of ZrO_2 nanoparticles that dissipated the electrical charge. About 7% ZrO_2 reinforced polymer nanocomposites exhibit three times higher values of dielectric constant than that of neat matrix, due to uniform distribution of ZrO_2 nanoparticles. The dielectric loss spectra over the measured frequency range of 1 Hz–1 MHz, that are represented in Figure 11(b). When compared with that of neat cyanate ester matrix, the ZrO_2 doped nanocomposite shows the considerably lower values of dielectric loss. The increase in ZrO_2 concentration increases the values of dielectric loss; however, it is still low for 10% ZrO_2 nanocomposites. The material with higher dielectric constant and lower dielectric loss is a desirable feature for ideal dielectric materials. In this view the developed cyanate ester was copolymerized with azomethine and ZrO_2, and they show higher dielectric constant and lower dielectric loss. The higher dielectric constant of the nanocomposites mainly attributed to the dispersion of highly polarizable ZrO_2 in the cyanate ester matrix. In addition, the copolymerization of azomethine with cyanate ester further increases the intrinsic dielectric features of the composites. Well dispersion of ZrO_2 leads to the interfacial polarizability which reduces the dielectric loss significantly. At higher ZrO_2 concentration, the aggregation of

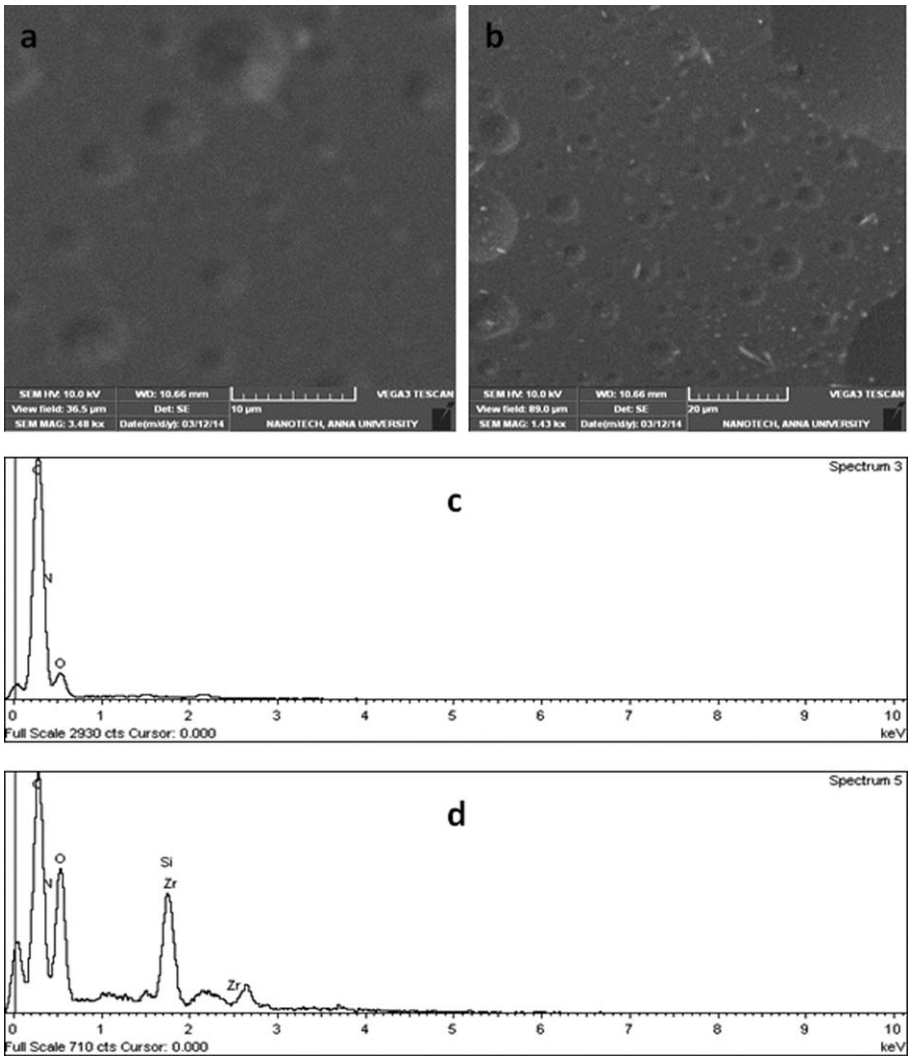

Figure 8. SEM images of Cy-OCN/AM-OH (**a**) and 7% Cy-OCN/AM-OH/ZrO_2 (**b**), and the corresponding EDS spectra of Cy-OCN/AM-OH (**c**) and 7% Cy-OCN/AM-OH/ZrO_2 (**d**) polymeric nanocomposites.

nanoparticles reduced the values of dielectric constant due to the blocking effect. This is because of poor particle dispersion and insufficient adhesion with polymer matrix that may cause the voids and pores within the composite that reduces the dielectric constant at higher ZrO_2 concentration.

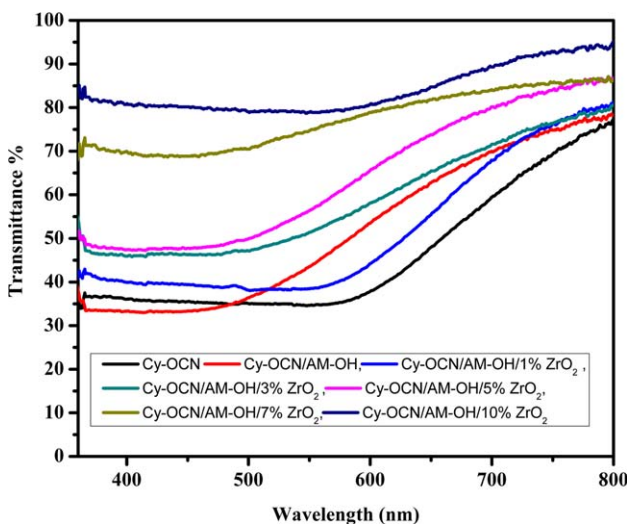

Figure 9. UV–visible spectra of Cy-OCN/AM-OH/ZrO_2 nanocomposite films. [Color figure can be viewed in the online issue, which is available at wileyonlinelibrary.com.]

Figure 12(a,b) represents the frequency dependency of dielectric constant (a) and dielectric loss (b) for Cy-OCN/AM-OH/ZrO_2 polymeric nanocomposites. From Figure 12(a) the significant variation on dielectric constant with the frequency as well as ZrO_2 concentration can be seen. There is no visible peak in the dielectric constant against frequency indicating homogeneous polarization process within the composites. Over the measured frequency region, plateau variation in dielectric constant was observed for all the composites except 7% ZrO_2 doped Cy-OCN/AM-OH/ZrO_2 composite. It shows two plateau regions for both lower and higher frequency polarization process which demonstrates that the low relaxation for 7% ZrO_2 doped polymer nanocomposite thereby increase the dielectric constant due to strong interfacial polarization.[22] Further increasing the ZrO_2 concentration to 10%, there may be the aggregation of inorganic fillers within the polymer and that limits the homogenous interaction at the polymer filler interface thus reduces the dielectric constant significantly by reducing the interfacial polarization. This result confirms the influence of both polymer and ceramic filler on the dielectric constant.[23] To further conclude the above results, the dielectric loss plot with respect to the ZrO_2 concentration is shown in Figure 12(b). It can be

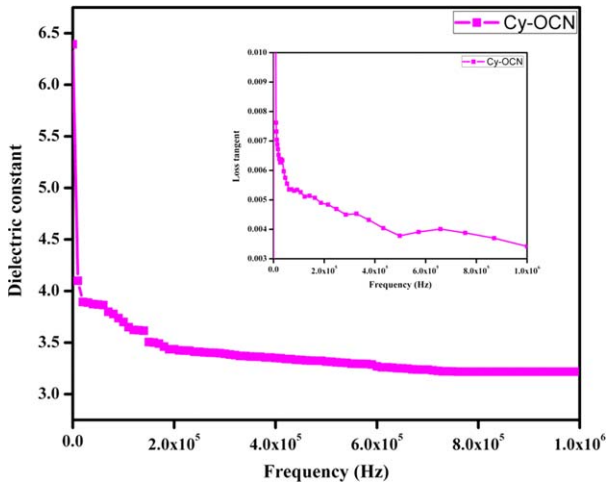

Figure 10. Dielectric constant of Cy-OCN, Dielectric loss of Cy-OCN. [Color figure can be viewed in the online issue, which is available at wileyonlinelibrary.com.]

understood that dominant dc conductivity at low frequency region for the composite at ambient temperature may be due to the addition of zirconia that enhances the hopping mechanism. The broad peak at high frequency describes the delayed relaxation process which facilitates high dielectric permittivity for all the composites.[22] Therefore the addition of ZrO_2 strongly influences the relaxation time, dielectric loss, and dielectric constant significantly.

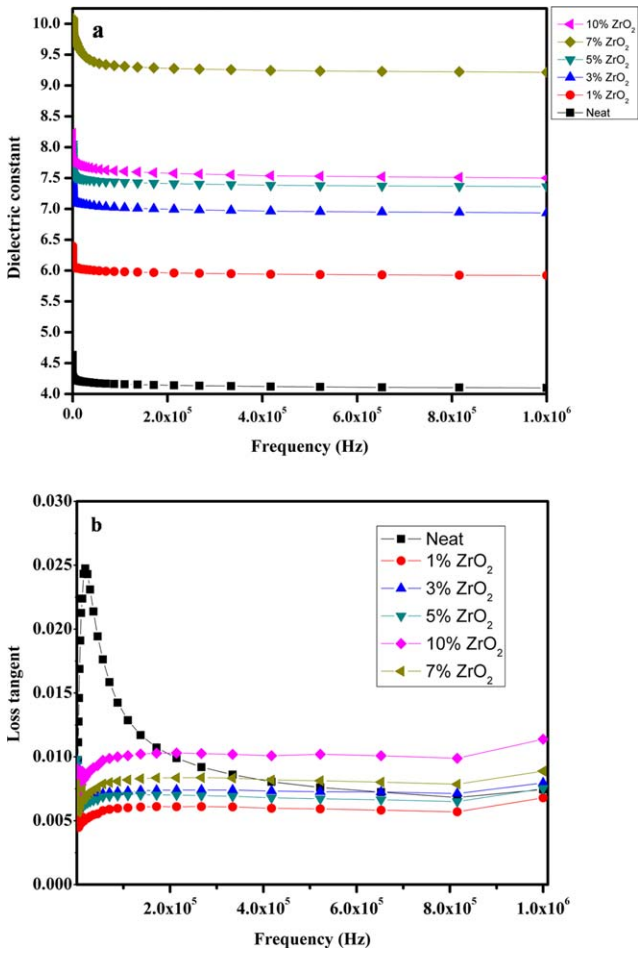

Figure 11. (**a**) Dielectric constant of polymer nanocomposites. (**b**) Dielectric loss of polymer nanocomposites. [Color figure can be viewed in the online issue, which is available at wileyonlinelibrary.com.]

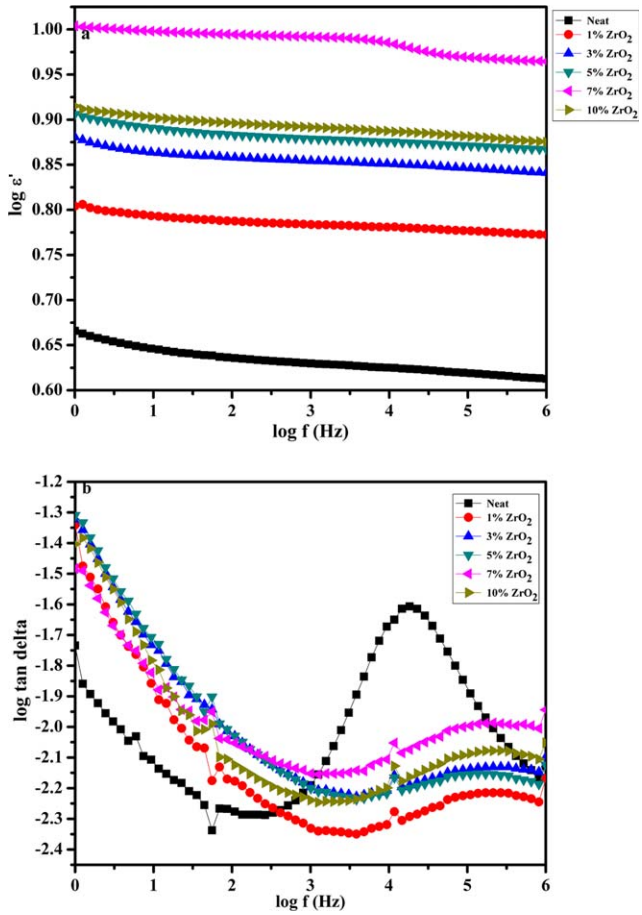

Figure 12. (**a**) Log–log plot of dielectric constant. (**b**) Log–log plot of dielectric loss. [Color figure can be viewed in the online issue, which is available at wileyonlinelibrary.com.]

CONCLUSION

The high k dielectric material has been developed via sol–gel technique based on cyanate-ester copolymerized with azomethine. The incorporation of ZrO_2 at various weight percentages to the polymer matrix tunes the values of dielectric constant to a significant extent. It was observed that the 7% ZrO_2 reinforced composite exhibit the maximum values of dielectric constant of 9.21 which is three times higher than that of neat cyanate-ester matrix. The well dispersion of ZrO_2 in the polymer matrix enhances the dielectric constant as well as the thermal stability of the resulting nanocomposites.

ACKNOWLEDGMENTS

The authors thank DST (Nanomission), SR/NM/NS-18/2010, New Delhi, Government of India, for the financial support and Dr. K. Gunasekaran and Mr. M. Kesavan, Department of Crystallography and Biophysics for providing NMR facility. The authors also thank Dr. S. Balakumar, National Centre for

Nanoscience and Nanotechnology, University of Madras, for providing HRTEM facility.

REFERENCES

1. Sasi kumar, R.; Ariraman, M.; Alagar, M. *RSC Adv.* **2014**, *4*, 19127.
2. Zhang, X.; Liang, G.; Chang, J.; Gu, A.; Yuan, L.; Zhang, W. *Carbon* **2012**, *50*, 4995.
3. Lu, J.; Moon, K. S.; Xu, J.; Wong, C. P. *J. Mater. Chem.* **2006**, *16*, 1543.
4. Selvi, M.; Vengatesan, M. R.; Prabunathan, P.; Song, J. K; Alagar, M. *Appl. Phys. Lett.* **2013**, *103*, 152902.
5. Chang, H. C.; Lin, H. T.; Lin, C. H. *Polym. Chem.* **2012**, *3*, 970.
6. Hamerton, I.; Emsley, A. M.; Howlin, B. J.; Klewpatinond, P.; Takeda, S. *Polymer* **2003**, *44*, 4839.
7. Corley, C. A.; Guenthner, A. J.; Sahagun, C. M.; Lamison, K. R.; Reams, J. T.; Hassan, M. K.; Morgan, Z. S. E.; Iacono, S. T.; Mabry, J. M. *ACS. Macro. Lett.* **2014**, *3*, 105.
8. Cao, L.; Zhang, W.; Zhang, X.; Yuan, L.; Liang, G.; Gu, A. *Ind. Eng. Chem. Res.* **2014**, *53*, 2661.
9. Wang, B.; Liang, G.; Jiao, Y.; Gu, A.; Liu, L.; Yuan, L.; Zhang, W. *Carbon* **2013**, *54*, 224.
10. Mi, Y.; Liang, G.; Gu, A.; Zhao, F.; Yuan, L. *Ind. Eng. Chem. Res.* **2013**, *52*, 3342.
11. Devaraju, S.; Vengatesan, M. R.; Selvi, M.; Ashok Kumar, A.; Hamerton, I.; Go, J. S.; Alagar, M. *RSC Adv.* **2013**, *3*, 12915.
12. Qi, W. J.; Nieh, R.; Lee, B. H.; Kang, L.; Jeon, Y.; Lee, J. C. *Appl. Phys. Lett.* **2000**, *77*, 3269.
13. Chandramohan, A.; Dinkaran, K.; Ashok Kumar, A.; Alagar, M. *High Perform. Polym.* **2012**, *24*(5), 405.
14. Devaraju, S.; Vengatesan, M. R.; Selvi, M.; Song, J. K.; Alagar, M. *Microp. Mesop. Mater.* **2013**, *179*, 157.
15. Chao, F.; Bowler, N.; Tan, X.; Liang, G.; Michael, R. *Compos. Part A* **2009**, *40*, 1266.
16. Dinakaran, K.; Alagar, M. *Polym. Adv. Technol.* **2003**, *14*, 544.
17. Pickup, D. M.; Mountjoy, G.; Wallidge, G. W; Newport, R. J.; Smith, M. E. *Phys. Chem. Chem. Phys.* **1999**, *1*, 2527.
18. Matthias, G. S.; Birgit, F; Hans, W. S.; Arne, T.; Xinliang, F.; Klaus, M. *J. Am. Chem. Soc.* **2009**, *131*, 7216.
19. I-Ann, L.; Dai-Fu, L.; Trong-Ming, D.; Wen-Chang, C.; Yang-Yen, Y.; Wen-Yen, C. *Mater. Chem. Phys.* **2014**, *144*, 41.
20. Meltem, A.; Esin, B.; Funda, S.; Nadir, K.; Ertuğrul, A. *J. Non-Crystal. Sol.* **2011**, *357*, 206.
21. Xie, L.; Huang, X.; Huang, Y.; Yang, K.; Jiang, P. *J. Phys. Chem. C* **2013**, *117*, 22525.
22. Gerhardt, R. *J. Phys. Chem. Solids* **1994**, *55*, 1491.
23. Popielarz, R.; Chiang, C. K.; Nozaki, R.; Obrzut, J. *Macromolecules* **2001**, *34*, 5910.